Published in final edited form as:
Ann Biomed Eng. 2014 July ; 42(7): 1546–1556. doi:10.1007/s10439-013-0937-9.

Experimental and Computational Investigation of Altered Mechanical Properties in Myocardium after Hydrogel Injection

Elena Tous Kichula[1], **Hua Wang**[3], **Shauna M. Dorsey**[1], **Spencer E. Szczesny**[1], **Dawn M. Elliott**[2], **Jason A. Burdick**[1,*], and **Jonathan F. Wenk**[3,4,*]

[1]Department of Bioengineering, University of Pennsylvania, Philadelphia, PA

[2]Department of Biomedical Engineering, University of Delaware, Newark, DE

[3]Department of Mechanical Engineering, University of Kentucky, Lexington, KY

[4]Department of Surgery, University of Kentucky, Lexington, KY

Abstract

The material properties of myocardium are an important determinant of global left ventricular function. Myocardial infarction results in a series of maladaptive geometric alterations which lead to increased stress and risk of heart failure. *In vivo* studies have demonstrated that material injection can mitigate these changes. More importantly, the material properties of these injectates can be tuned to minimize wall thinning and ventricular dilation. The current investigation combines experimental data and finite element modeling to correlate how injectate mechanics and volume influence myocardial wall stress. Experimentally, mechanics were characterized with biaxial testing and injected hydrogel volumes were measured with magnetic resonance imaging. Injection of hyaluronic acid hydrogel increased the stiffness of the myocardium/hydrogel composite region in an anisotropic manner, significantly increasing the modulus in the longitudinal direction compared to control myocardium. Increased stiffness, in combination with increased volume from hydrogel injection, reduced the global average fiber stress by ~14% and the transmural average by ~26% in the simulations. Additionally, stiffening in an anisotropic manner enhanced the influence of hydrogel treatment in decreasing stress. Overall, this work provides insight on how injectable biomaterials can be used to attenuate wall stress and provides tools to further optimize material properties for therapeutic applications.

Keywords

Hyaluronic Acid; Hydrogel; Finite Element Modeling; Left Ventricular Remodeling; Myocardial Infarction

[*]Co-Corresponding Authors: Jonathan F. Wenk, Ph.D. University of Kentucky Department of Mechanical Engineering 269 Ralph G. Anderson Building Lexington, KY 40506-0503 Phone: (859) 218-0658 Fax: (859) 257-3304 wenk@engr.uky.edu Jason A. Burdick, Ph.D. University of Pennsylvania Department of Bioengineering 102 Hayden Hall Philadelphia, PA Phone: (215) 898-8537 Fax: (215) 573-2071 burdick2@seas.upenn.edu.

Introduction

Increased stress due to left ventricular (LV) remodeling is thought to exacerbate the series of maladaptive events that ensue post-myocardial infarction (MI), potentially leading to heart failure.[3,5,8] As discussed by Holmes et al.,[12] during the ischemic phase of MI contractile function is impaired, or completely lost, and within a few hours of MI initiation the passive stiffness of the myocardium begins to increase. During the necrotic and fibrotic phases, dead tissue is removed due to an inflammatory response and replaced with collagen fibers. In the final remodeling phase, the wall thickness decreases and passive stiffness is also thought to decrease, which can both lead to global dilation and increased stress.

Injectable biomaterials, with their ability to limit geometric alterations, have become an attractive approach to decrease stress in the myocardial wall.[19,26] Several experimental studies have utilized large animal models of MI and treatment with various injectable materials (including Radiesse and hyaluronic acid (HA) hydrogels) in order to explore their impact on wall thickness and LV function.[13,18,25] It was found that material injection increased wall thickness and ejection fraction, relative to untreated infarcts. Studies utilizing HA hydrogel treatment delved more into the role of their material properties in limiting LV remodeling. This work demonstrated that the efficacy of material treatment in attenuating wall thinning and dilation was dependent on hydrogel mechanics[13,25] and degradation rate.[25] While these studies showed the influence of injectable materials in mitigating geometric alterations, no insight was provided on their exact role on the relationship of injectate properties in reducing wall stress. This is due to the difficulty in measuring forces in the myocardial wall *in vivo.*

In recent years, finite element (FE) models have been developed to better understand and examine the influence of material treatment on myocardial stress levels.[30,33] Utilizing a FE model to simulate injection of a non-contractile material into the myocardium, Wall et al. demonstrated that bulking (i.e., thickening) the myocardium was sufficient to attenuate stress in the myocardial wall post-MI.[11] Further investigations have demonstrated the relevance of injection volume and mechanics on the degree of stress reduction. Wenk et al. developed a FE model of a globally dilated LV that provided more control over injection characteristics, where in addition to the mechanical properties, inclusion (or injection) volume, geometry, and injection distribution in the LV could be adjusted.[13] The injection pattern resulted in a reduction in average global wall stress. However, the exact shape of the injection regions was not known in that study. In another study, Wenk et al. used a FE model of an infarcted LV to predict the changes in mechanical properties required to make a dyskinetic infarct become akinetic.[31] The result indicated that the stiffness needed to be increased by nearly 300 times, but this was only hypothetical.

Despite advances in FE models of injection treatment, there has yet to be direct comparison between experimental results and models to better understand how materials can influence stress behavior upon injection. In the current investigation we focus on the experimental generation of injection volume/shape data in LV explants using magnetic resonance imaging (MRI) and their mechanical properties using biaxial testing. As in previous work by Ifkovits et al.,[13] HA hydrogels were functionalized with a methacrylate to synthesize a

methacrylated HA (MeHA) macromer that was used for injection. The experimentally measured information was then employed directly in a FE model of an LV treated with an injection distribution pattern that was previously explored in an *in vivo* study,[13] to investigate stress levels based on experimentally derived, rather than theoretical input values. The model was developed to mimic the acute effects of hydrogel injection within a short time after an MI. This investigation will ultimately provide a better understanding of the relationship between injectate material properties (i.e., mechanics and volume) and stress reduction post-MI and insight on material design criteria for injectable biomaterials to attenuate LV remodeling.

Materials and Methods

Methacrylated Hyaluronic Acid (MeHA) Synthesis and Gelation

MeHA was synthesized as previously described (Figure 1A).[2] Briefly, methacrylic anhydride (MA, Sigma) was added to a 1 wt% solution of HA sodium salt (Lifecore, 66kDa) in deionized water maintained at pH 8 on ice. Excess unreacted MA was removed by dialysis (MW cutoff 5-8 kDa) against deionized water at room temperature (RT) for at least 3 days with repeated water changes. The final product was frozen, lyophilized, and stored in powder form at −20 °C until further use. Methacrylate coupling to HA and macromer purity were assessed via ^{1}H NMR (Bruker, 360 MHz). For gelation, the MeHA macromer was mixed and crosslinked with the redox chemical initiators ammonium persulfate (APS, 5 mM, Sigma) and tetramethylethylenediamine (TEMED, 5 mM, Sigma). Gelation was evaluated by monitoring the storage (G') and loss (G") modulus using an AR2000ex Rheometer (TA Instruments) at 37 °C under 1% strain and a frequency of 1 Hz in a cone and plate geometry (1°, 20 mm diameter, Figure 1B).

Non-Contrast Magnetic Resonance Imaging

Hydrogel distribution and volume within the myocardium was assessed by mimicking the experimental *in vivo* work of Ifkovits et al.[11] where 0.3 mL of the hydrogel formulation (4 wt% MeHA, 5 mM APS/TEMED in phosphate buffered saline (PBS)) was injected into explanted ovine LV myocardial tissue 3 minutes after mixing of the MeHA with initiators. The explanted ovine hearts were acquired from a local butcher shop. Thirty minutes later, the hydrogel/tissue samples were collected to include the entire injection region from the epicardium to endocardium. Injected explants were imaged using MRI without contrast agents by adjusting image parameters to exploit material intrinsic properties; a spin echo pulse sequence was employed and the echo time (30-60 ms) was adjusted for optimal contrast. Voxel size was also altered ($0.234 \times 0.234 \times 1.00$ mm^3 vs. $0.234 \times 0.234 \times 0.234$ mm^3) to optimize resolution. Final settings used for non-contrast imaging were as follows: echo time= 40 ms, repetition time= 5.8 s, matrix= $128 \times 128 \times 128$, field of view= 30×30 mm^2, voxel size = $0.234 \times 0.234 \times 0.234$ mm^3.

Explant samples were rinsed 6X at RT with 50 mL of sterile PBS (1% penicillin strepromycin (P/S)) and overnight for 3 days at 4 °C in 200 mL of sterile PBS with daily PBS changes. This washing period was to remove any uncrosslinked macromer, and pilot studies showed that injection of macromer without initiator and washing with this process

led to a signal with <5% difference in signal from control tissue. Images were converted into NIFTI files using imageJ software and converted to their correct dimensions with convert3D (c3D software). Contrast was quantified using ITK-SNAP after MRI bias correction was performed with an N4 algorithm.[23,27] Automatic segmentation was performed using Atropos (an ITK-based multivariate *n*-class open source segmentation algorithm distributed with ANTs)[1,28] to distinguish hydrogel from the background tissue and for initial segmentation. The input domain component included only the tissue portion of images, and N4 images were segmented using a smoothing factor of 0.1 (mrf 1.0, 1×1×1) and defining 3 tissues (i.e., 3 distinct regions of segmentation). A manual segmentation for crosslinked hydrogel was subsequently performed; Atropos results were employed as initial detection criterion and crosslinked hydrogel was defined as a percent change in intensity between HA and tissue above 7% (i.e., one standard deviation (SD) above the average change in intensity at day 3 in uncrosslinked studies).

Hematoxylin & eosin (H&E) staining was performed on hydrogel/tissue composites to confirm hydrogel incorporation. Thirty minutes after hydrogel injection, tissue was fixed in 4% formalin overnight and paraffin embedded using standard histological techniques. Samples were processed into 7 μm sections and stained with H&E.

Biaxial Testing

Biaxial testing is a physiologically relevant technique to assess the mechanical properties of anisotropic tissue such as myocardium.[4,14,18,22,34] Injected explant tissue samples were prepared as described above and a total of 5 samples were tested. Untreated myocardium was used as a control. Samples were collected from the mid-myocardial region and trimmed to ~7 × 7 mm^2 with a thickness of ~2 mm. Average thickness values were calculated to compute cross-sectional areas in order to determine the stress in each loading direction. The surface of each sample was speckle-coated with Verhoeff's stain for post-test tissue strain analysis with digital image correlation (Figure 2A). As a point of attachment for mechanical testing, finger-like grips[14] were made out of waterproof sandpaper (T214 Norton) (~75 × 5 mm^2) to allow for free expansion of sample edges (Figure 2B). The sandpaper was folded in half, and 3, 25 × 1 mm “fingers” were excised at the free end so that 6 “fingers” in total (3 on the top and 3 on the bottom) were formed. Grips were painted white to enhance contrast and glued (Locite 454) onto the bottom and top of each side of the tissue samples with about 1 mm overlap between the grip and tissue. Brass 0.5 mm markers were painted black for contrast and placed on the central “finger” section of each group (4 markers in total) (Figure 2A and B). Before testing, samples were equilibrated for ~1 hour in PBS at RT.

Silk (2-0) sutures were folded in half and secured through the free end of each sandpaper grip by metal hooks. The looped ends of the sutures were then hooked around the pulleys attached to the motors of a custom biaxial device.[20] Four independent motors (controlled by LabVIEW software) applied strain to the myocardial samples in both the circumferential and longitudinal directions, while a high-resolution digital camera with a telecentric lens (NT63-730, Edmund Optics) tracked the black markers on the middle tabs to track strains. Testing was performed by grip-to-grip strain control; all samples were preconditioned, exposed to a 1 hour hold, and then tested. Preconditioning included prestraining to 0.01

equibiaxial strain and then equibiaxially straining to 0.20 for 5 cycles at 0.10 strain/min. Immediately after preconditioning, samples were subjected to a 1 hour hold where no load was applied and samples were allowed to freely contract in both directions. The test protocol was identical to the preconditioning parameters; data and images from the final loading curve of each test were used for experimental data analysis.

All moduli calculations were based on orienting samples for tests according to their original orthogonal orientation in the myocardium. To calculate tissue strains, 2-D displacement maps were rendered using the speckle-coated surface via digital image correlation (Vic2D 2009, Correlated Solutions). A single deformation gradient tensor **F** was calculated from the displacement map of each image by finding the least-squares solution to the system of equations with a Matlab algorithm developed and described by Szczesny et al.[24] The deformation gradient tensor **F** for each image was used to compute the tissue Green-Lagrange strain in both the longitudinal and circumferential directions. Stress-tissue strain curves were obtained for each sample and then used to derive the nonlinear material parameters for FE modeling.

Material model and curve fitting

The material response of both the control myocardium and myocardium injected with hydrogel (hydrogel/tissue composite) was represented using a nearly incompressible, transversely isotopic, hyperelastic constitutive law, which is defined as[10]:

$$W=\frac{C}{2}\left(e^{b_f E_{ff}^2+b_t\left(E_{ss}^2+E_{nn}^2+E_{ns}^2+E_{sn}^2\right)+b_{fs}\left(E_{fs}^2+E_{sf}^2+E_{fn}^2+E_{nf}^2\right)}-1\right) \quad (1)$$

where C, b_f, b_t, and b_{fs} are the diastolic material parameters, and E_{ij} are the components of the Green-Lagrange strain tensor relative to the myofiber coordinate system (f = fiber direction, s = cross-fiber in-plane direction, n = transverse-fiber direction). In the case of myocardium injected with hydrogel, it was assumed that the gel was evenly dispersed within the sample. Thus, rather than representing the myocardium and hydrogel with separate constitutive laws, it was assumed that the "effective" response of the hydrogel/tissue composite material could be represented with the constitutive law in Eqn (1). This results in altered material parameters that represent the influence of the gel on modifying myocardial stiffness.

During planar biaxial testing the deformation is limited to stretching along two primary loading directions. When controlled properly, the shear deformation is minimal compared to the normal components, and thus can be ignored. For this type of deformation, the stress can be posed in terms of the stretch ratios in the primary loading directions. Using the assumption of plane stress, due to the sample thickness, and the fact that the myofibers were oriented in the primary stretching direction, the Cauchy stress can be defined as

$$\sigma_{11}=\frac{C}{2}e^{\frac{b_f}{4}\left(\lambda_1^2-1\right)^2+\frac{b_t}{4}\left(\left(\lambda_2^2-1\right)^2+\left(\frac{1}{\lambda_1^4\lambda_2^4}-1\right)^2\right)}\left(b_f\left(\lambda_1^4-\lambda_1^2\right)-b_t\left(\frac{1}{\lambda_1^4\lambda_2^4}-\frac{1}{\lambda_1^2\lambda_2^2}\right)\right) \quad (2a)$$

$$\sigma_{22}=\frac{C}{2}e^{\frac{b_f}{4}\left(\lambda_1^2-1\right)^2+\frac{b_t}{4}\left(\left(\lambda_2^2-1\right)^2+\left(\frac{1}{\lambda_1^4\lambda_2^4}-1\right)^2\right)}\left(b_t\left(\lambda_1^4-\lambda_1^2-\frac{1}{\lambda_1^4\lambda_2^4}+\frac{1}{\lambda_1^2\lambda_2^2}\right)\right) \quad (2b)$$

where σ_{11} and λ_1 are the stress and stretch ratio in the circumferential (myofiber) direction, respectively, and σ_{22} and λ_2 are the stress and stretch ratio in the longitudinal (cross-fiber in-plane) direction, respectively. The stretch ratios and normal components of Green-Lagrange strain are related by $E_{ii}=\frac{1}{2}\left(\lambda_i^2-1\right)$, where i=1,2,3.

Biaxial data from the control and hydrogel/tissue composite experiments were fit to the stress-stretch relation defined in Eqn (2). A Genetic Algorithm was employed to determine the optimal set of material parameters (C, b_f, b_t) that minimized the difference between the predicted and experimental stress-strain curves, i.e., the value of ($R^2 - 1$) was minimized for each set of curves, where R^2 is the coefficient of determination. A Genetic Algorithm is an intelligent searching technique that is used to probe a desired parameter space in order to minimize an objective function without the need for taking the gradient of that function. Since the shear deformation was negligible, only the parameters C, b_f, and b_t were determined from the biaxial stretching experiments.

Finite Element Model of a Left Ventricle with Injections

In order to determine the influence of hydrogel injections on myocardial wall stress, two different FE models of a LV were generated, one with and one without injections. The geometry of the LV wall was based on experimental measurements from the normal ovine hearts used in this study. For the control case, the wall thickness was approximately 1.3 cm near the equator of the LV and 0.8 cm near the apex. The inner diameter of the endocardial wall near the equator was 4 cm, while the distance from apex to base was 6.4 cm. The myofiber orientation was assigned to vary linearly from epicardium to endocardium using the angles of −37 degrees to 83 degrees, respectively. The material properties of the LV wall were based on the curve fitting results from the experimental biaxial testing of control myocardium.

In order to account for the presence of the hydrogel, the control model was modified to include a pattern of 20 hydrogel/tissue composite regions around the free wall (Figure 3A). The number of regions was based on work by Ifkovits et al.,[11] where 20 injections of hydrogel were made into an ovine anteroapical infarct. In that work, the injections were made 30 minutes after the MI was induced. According to Holmes et al.,[12] the passive properties of the myocardium begin to stiffen 4 to 6 hours post-MI. Since the model is meant to mimic the initial time frame after infarction, it is assumed that 30 minutes post-MI the properties would be roughly unchanged. Hence, the model was created such that the properties around the hydrogel/tissue composite regions were the same as the control case. The size and shape of the hydrogel/tissue composite regions were based on the MR images of injected explant tissue, which are given in the Results section. The wall thickness around the hydrogel/tissue composite regions was increased to account for the volume added to the wall, thus preserving the volume of myocardium (Figure 3B and 3C). Since each injection

was 0.3 mL, the total amount of volume added to the model was 6 mL. This led to an increase in wall thickness of approximately 1.4 mm within the model. The LV wall away from the injections, and the longitudinal dimensions were unaltered relative to the control case. The material properties of the hydrogel/tissue composite regions were based on the curve fitting results from the experimental biaxial testing of samples taken from the center of the ellipsoidal composite site. It should be noted that the value for b_{fs} was based on the literature, since it cannot be determined from biaxial testing, and was assigned to be 12.[29]

Statistical Analysis

Data are presented as mean ± SEM, as indicated in the figure legend. Changes in data were assessed using a 2- sample t-test and assuming equal variances. $p < 0.05$ was considered statistically significant for all comparisons.

Results

MeHA Hydrogel Formation and Characterization

MeHA functionalization was assessed via ^{1}H NMR by integrating the acrylate peaks resonating at δ ~6.10 ppm and δ ~5.70 ppm to the HA backbone and was confirmed to be ~60% for the macromer used in this study. The redox initiators APS and TEMED were employed at 5 mM for hydrogel formation of a 4 wt% MeHA solution in PBS. Gelation was monitored with rheometry and gel onset was determined to be 234±6 seconds, where gel onset was defined as the intersection of G' and G" (Figure 1B). The hydrogel modulus reached a plateau within 30 minutes.

Non-Contrast MRI

The proton makeup of a water swollen HA hydrogel is different from that of tissue; thus, when injected into an explant, the endogenous properties of the composite hydrogel/tissue region are different compared to tissue alone. It is not completely understood how much of this is due to changes in proton density or relaxation times, yet hydrogels are detectable without the inclusion of contrast agents. Initial studies were performed to understand whether the injected macromer would be present in the tissue, if it is not crosslinked into the gel. To address this, MeHA was injected into explants without initiator and washed for up to 5 days. After 3 days, there were negligible differences between the control tissue and the tissue washed free of macromer (Figure 4A).

Figure 4A illustrates that, compared to minimal contrast observed in control myocardial tissue, the tissue-embedded MeHA formulation was clearly distinguishable. While the geometry of injections varied somewhat, most injections took on an ellipsoidal shape with the major axis matching the fiber direction. The longitudinal (X_l) and circumferential (X_c) axes of the composite region are shown in Figure 4A, and the full ellipsoid can be seen clearly in the 3D rendering of the composite region (Figure 4B). The dimensions and volumes of the 4 composite samples were estimated from the imaging data. The average length in the circumferential, longitudinal, and transmural directions was found to be 1.725±0.25 cm, 0.575±0.15 cm, and 0.875±0.096 cm, respectively, and the volume was 0.420±0.162 mL. It should be noted that in most cases, calculated volumes were larger than

the original 0.3 mL that was injected, suggesting that the hydrogel is dispersing within the tissue. While hydrogels did at times form small hydrogel "plugs" (areas of mostly hydrogel), they generally dispersed nicely within the fibers (Figure 4C). The smallest dimension of the hydrogel/tissue composite region was in the longitudinal direction. This is most likely due to the sheet structure of the myocardium, causing the hydrogel to disperse between layers.

Biaxial Testing

Biaxial testing was conducted on control myocardium (n=5) and hydrogel/tissue composite (n=5) samples. The resulting stress-strain curves were then fit in order to determine the parameters for the constitutive model in Eqn (2). Experimental stress-strain points from a control and composite experiment are shown in Figure 5A, along with the corresponding curve fit. All of the parameters from the curve fitting procedure are reported in Table 1A and 1B for the control and composite case, respectively. Note that there was good agreement between the experimental and curve fit results for both the control and composite cases. The average parameters for each case are given in Table 1C. These values were plugged into Eqn (2) in order to generate the representative biaxial stress-strain curves shown in Figure 5B. It can be seen that the composite was stiffer than the control (Figure 5B) in both loading directions and that the anisotropy was reduced, i.e., the difference in directional stiffness is reduced.

In order to further explore the changes in anisotropy, the directional "modulus" in different strain ranges was examined. This was approximated to be the change in stress over each of the strain ranges. Myocardial physiological strain has been reported to range from 0.10 to 0.15;[7,11,16,21] to account for the lower and higher ends, a mechanical assessment was performed between 0.05 and 0.10 and between 0.10 and 0.15 Green-Lagrange strain, where 0.05-0.10 corresponded to the linear toe region in stress-strain curves (Figure 6A and 6B). A strain range of 0.15-0.20 (Figure 6A and 6B), which generally corresponded to the second linear portion in stress-strain curves, was analyzed as an extreme case that could potentially represent a hypertrophied borderzone. Overall, when compared to control myocardium, a directionally dependent trend was observed where moduli were influenced most in the longitudinal direction. Results demonstrated that in the longitudinal direction, the moduli of hydrogel/tissue composite samples were higher than in control myocardium specimens in all Green-Lagrange strain ranges with significant changes observed at 0.10-0.15 (56.8 vs. 9.9 kPa, respectively). This trend was not as distinct in the circumferential direction, where moduli of the hydrogel/tissue samples were slightly higher between 0.05-0.10 and 0.15-0.20 and comparable to control myocardium between 0.10-0.15.

Overall, tissue strain analysis data indicates that hydrogel incorporation influences the mechanics of the myocardial tissue, generally resulting in larger increases in stiffness in the longitudinal direction than in the circumferential direction. As a result, the anisotropic ratio (circumferential/longitudinal) for the composite formulation was decreased compared to control myocardium in all Green-Lagrange strain ranges, Figure 6C; a significant decrease was observed at 0.10-0.15 (1.7 vs. 8.1, respectively).

FE Modeling Stress Analysis

The FE models for the control and hydrogel injected LV cases were both simulated using an end-diastolic pressure of 10 mmHg as a boundary condition on the endocardial surface. The material parameters were assigned using the average values from the biaxial testing (Table 1C). Diastolic stress in the fiber direction was calculated using a volume average over several regions, in order to assess the local and global effects of the hydrogel injections. The average stress results are given in Table 2. Note that the global average was calculated using all of the elements in the LV mesh, the circumferential average used the elements boxed in Figure 3C, the longitudinal average used the elements boxed in Figure 3B, and the transmural average used the elements in and around the injection site shown in Figure 3A with the arrow. The global average of fiber stress was reduced by roughly 14% due to the presence of the injections. The transmural average, which represents a local change in stress, was reduced by 26%. The stress distribution within the LV wall for the hydrogel injected case is shown in Figure 7. Note that the endocardial and midmyocardial stresses were reduced, due to the presence of the hydrogel.

In order to assess the influence of mechanical properties versus wall thickening, since hydrogel injection induces both, simulations were conducted where the properties of the composite regions were assigned to be the same as the control myocardium. Therefore, only wall thickening effects altered the stress distribution. It can be seen that the reduction in stress is 10.4% for the global average and 19.9% for the transmural average (Table 2). Thus, increased stiffness, due to the hydrogel injection, reduces the stress more than just thickening the ventricle wall alone.

Since the hydrogel also influences the anisotropy, simulations were conducted where the cross-fiber stiffness parameter (b_t) was varied while the fiber stiffness parameter (b_f) was held constant. This was done by altering the average composite parameters. When b_t was assigned to be 1, the fiber stress increased by 6%, whereas when b_t was assigned to be equal to b_f, the fiber stress decreased by 11%. Thus, as cross-fiber stiffness increases (reducing anisotropy) the fiber stress decreases even further.

Discussion

This study assessed the influence of hydrogel injection within the wall of normal myocardium on LV wall stress using experimental measurements of hydrogel/tissue composite sites to build a realistic FE model. To our knowledge, this is the first time that MRI has been used to evaluate the shape and distribution of hydrogel in the wall of myocardium and to use experimentally measured parameters of hydrogel injection for inputs to an FE model. The results indicate that the injected hydrogel increases mechanical stiffness in the longitudinal direction and reduces stress along the fiber direction.

Other FE studies have investigated the influence of injecting non-contractile material into the LV wall. Kortsmit et al. developed an FE model of an anteroapical infarct that was treated with hydrogel injection.[15] In that work, it was assumed that the hydrogel and tissue took on a discrete layered structure within the infarcted region, with the hydrogel and tissue alternating layers. This was based on histological sections of the treated infarct region.

Wenk et al. developed an FE model of an LV with dilated cardiomyopathy that was treated with spherical injection regions.[33] The injection sites were assumed to be discrete inclusions of pure Alginate.

In both studies, the LV wall stress was reduced due to the injected material, but the interaction of the hydrogel and tissue was not considered.

In the current study, the biaxial testing data indicates that hydrogel incorporation does influence the stiffness of myocardial tissue, generally resulting in a larger mechanical influence in the longitudinal direction than in the circumferential direction compared to control myocardium. Consequently, the anisotropy for the hydrogel formulation compared to control myocardium was decreased as indicated in Figure 6C. Healthy normal myocardial tissue is anisotropic; stiffness in one direction (circumferential) is higher than the other (longitudinal) direction.[7,10,34] The results reported in Figure 6 support this trend for normal myocardial tissue; however, when compared to control myocardium, hydrogel incorporation resulted in decreased anisotropy compared to control myocardium (Figure 6C). As hydrogels exhibit isotropic properties alone, this is not entirely unexpected as the composite consists of both cardiac tissue and hydrogel. Yet, this is interesting considering the recent findings of Fomovsky et al., which indicated that anisotropic stiffening may be beneficial in cardiac function.[9] Morita et al. observed a similar trend where treatment with their injectable dermal filler led to increased stiffening in the longitudinal direction.[18] It should be noted, however, that both of the aforementioned studies were performed in an infarct model, while this work was performed in normal myocardial tissue and this could influence the final outcomes. Regardless, this provides insight on the influence of injectable biomaterials on the mechanical properties (i.e., directional stiffening) of the myocardium.

Other approaches have also been developed to potentially reduce myocardial stress post-MI, thus reducing the adverse effects of remodeling. These include cardiac restraint devices, such as epicardial patches and wraps. In the study by Liao et al.,[17] localized synthetic patches were sutured to the epicardium over an MI in a pig model. In the study by Dvir et al.,[6] bioengineered patches were pre-vascularized via heterotopic transplantation onto the omentum. The patches were then explanted and transplanted onto the epicardium of an MI in a rat model. The results of both studies showed a reduction in MI wall thinning and an improvement in LV ejection fraction, relative to infarcted controls. Devices that wrap completely around the epicardium, and are made of synthetic materials, have been investigated and found to acutely reduce wall stress at the expense of reducing pump function.[32]

The modeling results in the current study show a clear reduction of stress based on the injection of a hydrogel formulation and experimentally measured parameters of volume and mechanics. However, the findings are based on a single formulation, which was previously injected into an ovine infarct model and showed positive findings with respect to infarct expansion and cardiac function. Thus, there is correlation between the current study, which predicts decreased stress and potential *in vivo* findings. As mentioned in the Introduction, there are a wide range of materials that have been injected into the myocardium and with some systems there is tunability in properties. For example, by tuning the stiffness of the

formulation, further reductions in stress may be achieved. The current results indicate that a formulation that is stiffer overall, and provides additional stiffening in the longitudinal direction, will reduce stress further. Thus, further experiments could correlate materials with varied properties using this approach.

One limitation of the current study is that it only focused on changes in passive stiffness due to hydrogel injection. Further studies are needed to assess changes in stress during systolic contraction. Additionally, features such as dispersion of the hydrogel might be different in a myocardial infarction versus normal myocardium used here; thus, further studies are required to assess this difference.

Conclusions

Myocardium injected with hydrogel was assessed using MRI and biaxial testing. The results of the MRI show that the hydrogel dispersed within the tissue, forming an ellipsoidal shape. Biaxial testing showed altered stiffness due to the hydrogel, which changed the anisotropy and increased the longitudinal stiffness. A FE model was generated using the experimentally determined material properties and injection geometry. The model predicted a reduction in local and global myofiber stress, with additional attenuation when the hydrogel/tissue stiffness was increased, indicating the need for further tuning of hydrogel properties. Overall, this work further advances the field and provides insight on how to improve material design of injectable biomaterials used to attenuate increased stress due to LV remodeling.

Acknowledgments

The authors acknowledge Daniel Adler in assisting with the analysis of the MRI images. This work was supported by the National Institutes of Health (R01 HL111090, T32 HL007954).

References

1. Avants BB, Tustison NJ, Wu J, Cook PA, Gee JC. An open source multivariate framework for n-tissue segmentation with evaluation on public data. Neuroinformatics. 2011; 9(4):381–400. [PubMed: 21373993]
2. Burdick JA, Chung C, Jia X, Randolph MA, Langer R. Controlled degradation and mechanical behavior of photopolymerized hyaluronic acid networks. Biomacromolecules. 2005; 6(1):386–391. [PubMed: 15638543]
3. Dang AB, Guccione JM, Mishell JM, Zhang P, Wallace AW, Gorman RC, Gorman JH 3rd, Ratcliffe MB. Akinetic myocardial infarcts must contain contracting myocytes: Finite-element model study. Am J Physiol Heart Circ Physiol. 2005; 288(4):H1844–1850. [PubMed: 15604126]
4. Demer LL, Yin FC. Passive biaxial mechanical properties of isolated canine myocardium. J Physiol. 1983; 339:615–630. [PubMed: 6887039]
5. Dobaczewski M, Gonzalez-Quesada C, Frangogiannis NG. The extracellular matrix as a modulator of the inflammatory and reparative response following myocardial infarction. J Mol Cell Cardiol. 2010; 48(3):504–511. [PubMed: 19631653]
6. Dvir T, Kedem A, Ruvinov E, Levy O, Freeman I, Landa N, Holbova R, Feinberg MS, Dror S, Etzion Y, Leor J, Cohen S. Prevascularization of cardiac patch on the omentum improves its therapeutic outcome. Proc Natl Acad Sci U S A. 2009; 106(35):14990–14995. [PubMed: 19706385]

7. Engelmayr GC Jr. Cheng M, Bettinger CJ, Borenstein JT, Langer R, Freed LE. Accordion-like honeycombs for tissue engineering of cardiac anisotropy. Nat Mater. 2008; 7(12):1003–1010. [PubMed: 18978786]
8. Epstein FH, Yang Z, Gilson WD, Berr SS, Kramer CM, French BA. Mr tagging early after myocardial infarction in mice demonstrates contractile dysfunction in adjacent and remote regions. Magn Reson Med. 2002; 48(2):399–403. [PubMed: 12210951]
9. Fomovsky GM, Macadangdang JR, Ailawadi G, Holmes JW. Model-based design of mechanical therapies for myocardial infarction. J Cardiovasc Transl Res. 2011; 4(1):82–91. [PubMed: 21088945]
10. Guccione JM, McCulloch AD, Waldman LK. Passive material properties of intact ventricular myocardium determined from a cylindrical model. J Biomech Eng. 1991; 113(1):42–55. [PubMed: 2020175]
11. Gupta V, Grande-Allen KJ. Effects of static and cyclic loading in regulating extracellular matrix synthesis by cardiovascular cells. Cardiovasc Res. 2006; 72(3):375–383. [PubMed: 17010955]
12. Holmes JW, Borg TK, Covell JW. Structure and mechanics of healing myocardial infarcts. Annu Rev Biomed Eng. 2005; 7:223–253. [PubMed: 16004571]
13. Ifkovits JL, Tous E, Minakawa M, Morita M, Robb JD, Koomalsingh KJ, Gorman JH 3rd, Gorman RC, Burdick JA. Injectable hydrogel properties influence infarct expansion and extent of postinfarction left ventricular remodeling in an ovine model. Proc Natl Acad Sci U S A. 2010; 107(25):11507–11512. [PubMed: 20534527]
14. Jacobs NT CD, Szczesny SE, Vresilovic EJ, Elliott DM. Effect of boundary conditions on stress-strain uniformity in biaxial tension of annulus fibrosus. Annual Meeting of the Orthopaedic Research Society. 2011
15. Kortsmit J, Davies NH, Miller R, Macadangdang JR, Zilla P, Franz T. The effect of hydrogel injection on cardiac function and myocardial mechanics in a computational post-infarction model. Comput Methods Biomech Biomed Engin. 2012
16. Lee AA, McCulloch AD. Multiaxial myocardial mechanics and extracellular matrix remodeling: Mechanochemical regulation of cardiac fibroblast function. Adv Exp Med Biol. 1997; 430:227–240. [PubMed: 9330732]
17. Liao SY, Siu CW, Liu Y, Zhang Y, Chan WS, Wu EX, Wu Y, Nicholls JM, Li RA, Benser ME, Rosenberg SP, Park E, Lau CP, Tse HF. Attenuation of left ventricular adverse remodeling with epicardial patching after myocardial infarction. J Card Fail. 2010; 16(7):590–598. [PubMed: 20610235]
18. Morita M, Eckert CE, Matsuzaki K, Noma M, Ryan LP, Burdick JA, Jackson BM, Gorman JH 3rd, Sacks MS, Gorman RC. Modification of infarct material properties limits adverse ventricular remodeling. Ann Thorac Surg. 2011; 92(2):617–624. [PubMed: 21801916]
19. Nelson DM, Ma Z, Fujimoto KL, Hashizume R, Wagner WR. Intra-myocardial biomaterial injection therapy in the treatment of heart failure: Materials, outcomes and challenges. Acta Biomater. 2011; 7(1):1–15. [PubMed: 20619368]
20. O'Connell GD, Sen S, Elliott DM. Human annulus fibrosus material properties from biaxial testing and constitutive modeling are altered with degeneration. Biomech Model Mechanobiol. 2011; 11(3-4):493–503. [PubMed: 21748426]
21. Rappaport D, Adam D, Lysyansky P, Riesner S. Assessment of myocardial regional strain and strain rate by tissue tracking in b-mode echocardiograms. Ultrasound Med Biol. 2006; 32(8):1181–1192. [PubMed: 16875953]
22. Sacks M. Biaxial mechanical evaluation of planar and biological materials. Journal of Elasticity. 2001; 61:199–246.
23. Sled JG, Zijdenbos AP, Evans AC. A nonparametric method for automatic correction of intensity nonuniformity in mri data. IEEE Trans Med Imaging. 1998; 17(1):87–97. [PubMed: 9617910]
24. Szczesny SE, Peloquin JM, Cortes DH, Kadlowec JA, Soslowsky LJ, Elliott DM. Biaxial tensile testing and constitutive modeling of human supraspinatus tendon. J Biomech Eng. 2012; 134(2): 021004. [PubMed: 22482671]
25. Tous E, Ifkovits JL, Koomalsingh KJ, Shuto T, Soeda T, Kondo N, Gorman JH 3rd, Gorman RC, Burdick JA. Influence of injectable hyaluronic acid hydrogel degradation behavior on infarction-

induced ventricular remodeling. Biomacromolecules. 2011; 12(11):4127–4135. [PubMed: 21967486]

26. Tous E, Purcell B, Ifkovits JL, Burdick JA. Injectable acellular hydrogels for cardiac repair. J Cardiovasc Transl Res. 2011; 4(5):528–542. [PubMed: 21710332]
27. Tustison NJ, Avants BB, Cook PA, Zheng Y, Egan A, Yushkevich PA, Gee JC. N4itk: Improved n3 bias correction. IEEE Trans Med Imaging. 2010; 29(6):1310–1320. [PubMed: 20378467]
28. Vannier MW, Butterfield RL, Jordan D, Murphy WA, Levitt RG, Gado M. Multispectral analysis of magnetic resonance images. Radiology. 1985; 154(1):221–224. [PubMed: 3964938]
29. Walker JC, Ratcliffe MB, Zhang P, Wallace AW, Fata B, Hsu EW, Saloner D, Guccione JM. Mri-based finite-element analysis of left ventricular aneurysm. Am J Physiol Heart Circ Physiol. 2005; 289(2):H692–700. [PubMed: 15778283]
30. Wall ST, Walker JC, Healy KE, Ratcliffe MB, Guccione JM. Theoretical impact of the injection of material into the myocardium: A finite element model simulation. Circulation. 2006; 114(24): 2627–2635. [PubMed: 17130342]
31. Wenk JF, Eslami P, Zhang Z, Xu C, Kuhl E, Gorman JH 3rd, Robb JD, Ratcliffe MB, Gorman RC, Guccione JM. A novel method for quantifying the in-vivo mechanical effect of material injected into a myocardial infarction. Ann Thorac Surg. 2011; 92(3):935–941. [PubMed: 21871280]
32. Wenk JF, Ge L, Zhang Z, Mojsejenko D, Potter DD, Tseng EE, Guccione JM, Ratcliffe MB. Biventricular finite element modeling of the acorn corcap cardiac support device on a failing heart. Ann Thorac Surg. 2013; 95(6):2022–2027. [PubMed: 23643546]
33. Wenk JF, Wall ST, Peterson RC, Helgerson SL, Sabbah HN, Burger M, Stander N, Ratcliffe MB, Guccione JM. A method for automatically optimizing medical devices for treating heart failure: Designing polymeric injection patterns. J Biomech Eng. 2009; 131(12):121011. [PubMed: 20524734]
34. Yin FC, Strumpf RK, Chew PH, Zeger SL. Quantification of the mechanical properties of noncontracting canine myocardium under simultaneous biaxial loading. J Biomech. 1987; 20(6): 577–589. [PubMed: 3611134]

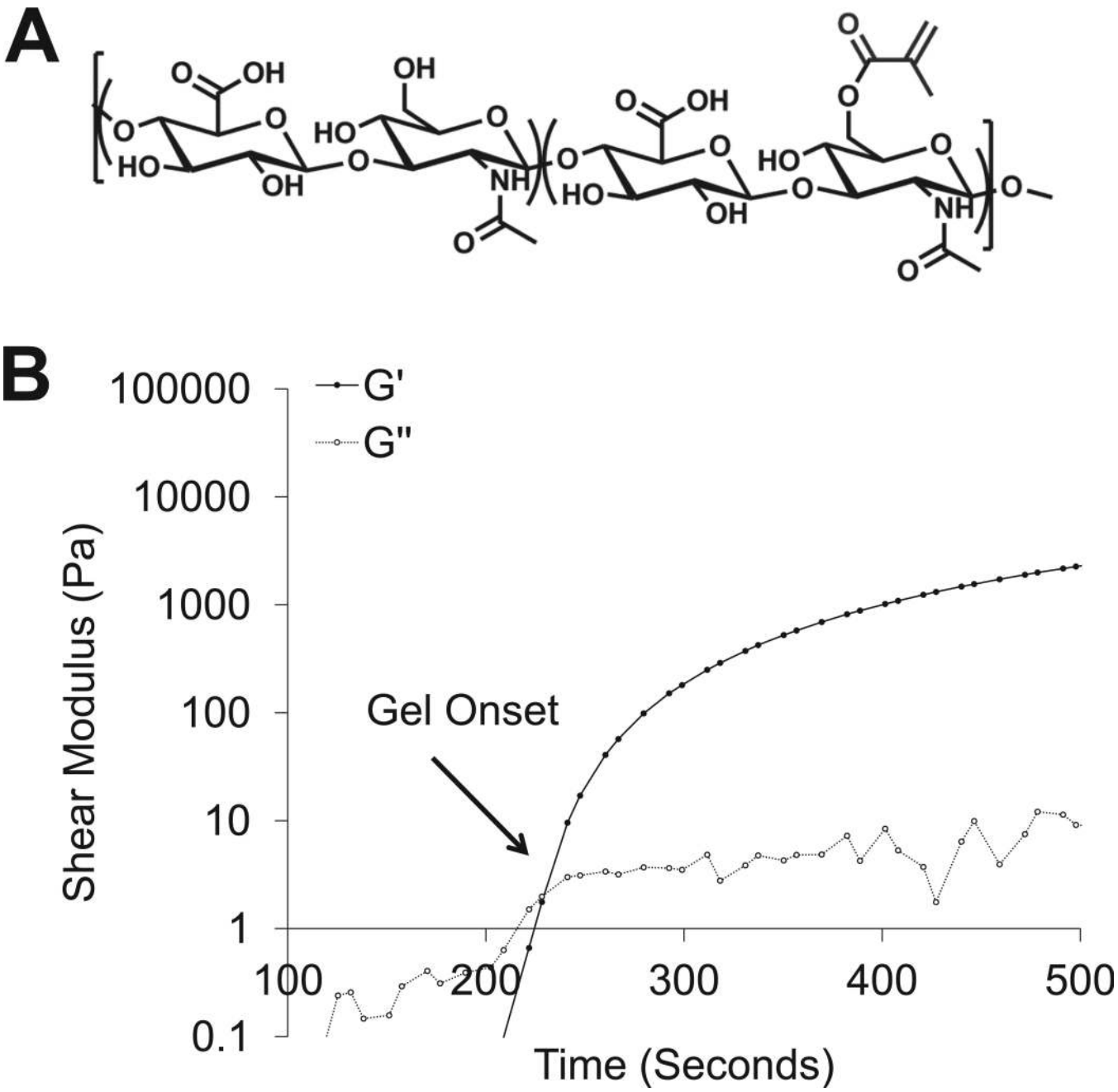

Figure 1.

(A) Chemical structure of methacrylated hyaluronic acid (MeHA) and (B) representative rheological time sweep, where the intersection of the storage (G') and loss (G") moduli is defined as the gel onset.

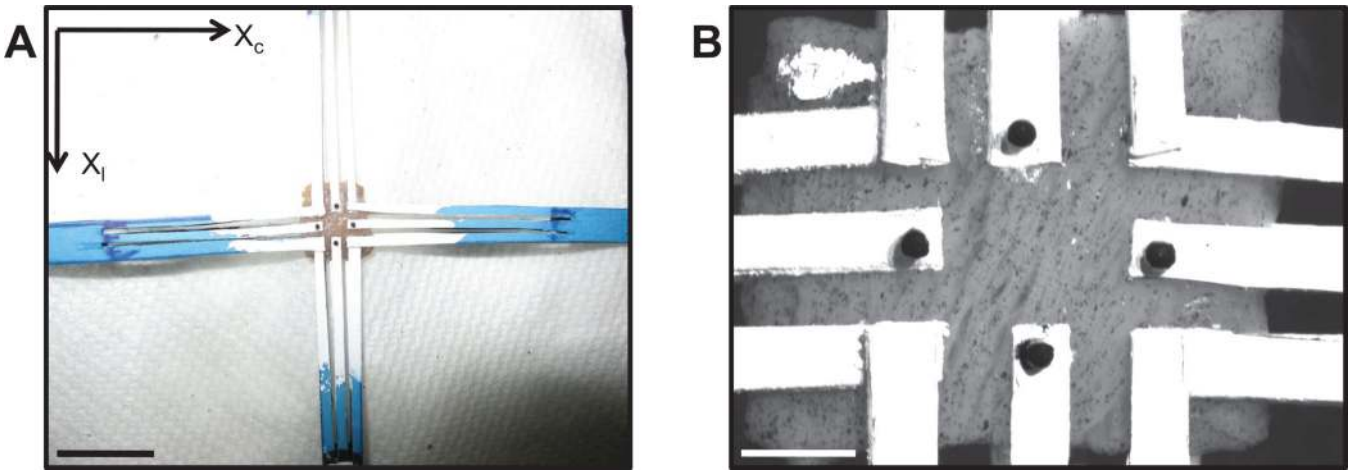

Figure 2.

Representative images of biaxial sample preparation. (A) Overhead view of specimen ready for biaxial mounting. (B) Zoomed in view of speckle-coated hydrogel/tissue composite (with finger-like grips and tracking markers) mounted on biaxial apparatus at 0 grip-to-grip strain. Scale bar =10 mm for (A) and scale bar = 1.5 mm for (B). (X_l: longitudinal axis and X_c: circumferential axis)

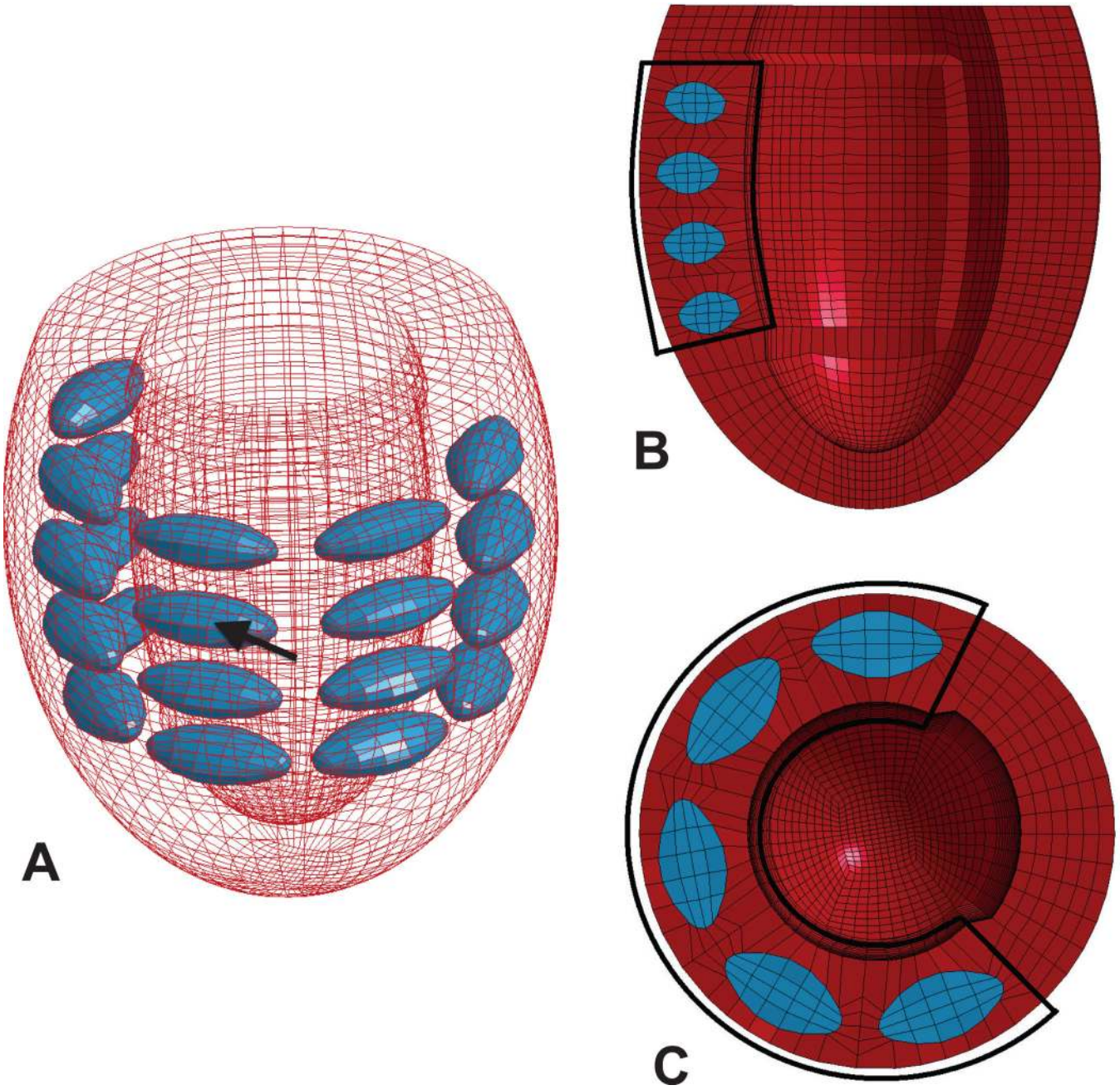

Figure 3.

(A) LV model with 20 injection sites, note the injection sites have the geometry and material properties of the hydrogel/tissue composite. (B) Long axis interior view with half the model removed, note the wall thickening around the injection sites. (C) short axis interior view with half the model removed, again note the thickening around the injection sites. The black boxes in (B) and (C) indicate the longitudinal and circumferential regions where average fiber stress was calculated, respectively.

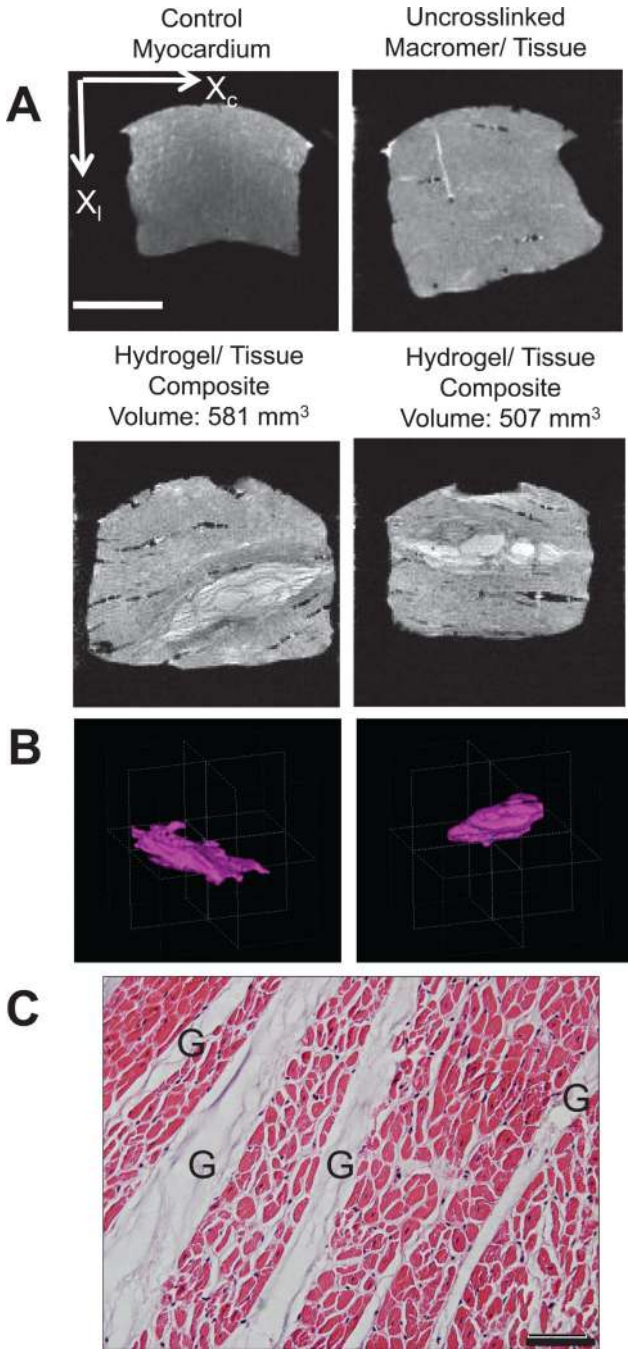

Figure 4.

(A) Representative MRI slice of control myocardium, myocardium with uncrosslinked macromer, and hydrogel/tissue composite samples (2 shown) at Day 3. (B) Respective 3-D construction of the injected hydrogels. (C) Representative H&E image of hydrogel dispersed in myocardial tissue (G = gel). Scale bar = 1 cm for (A) and 50 um for (B). (X_l: longitudinal axis and X_c: circumferential axis).

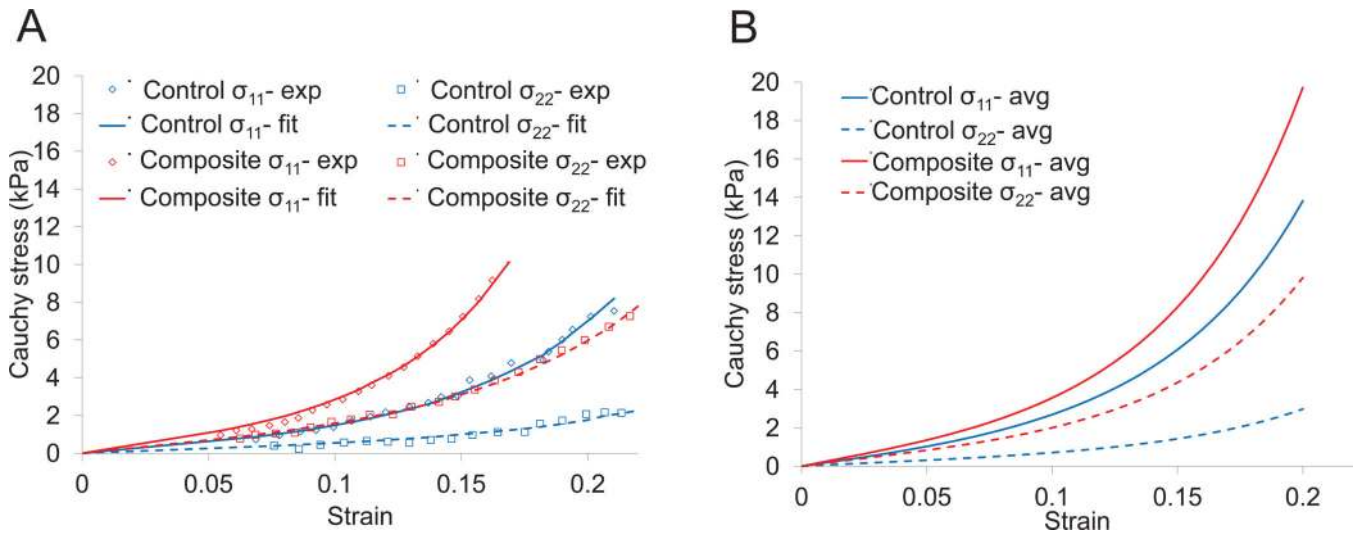

Figure 5.

(A) Curve fit results for representative samples of control myocardium and hydrogel/tissuel composite. (B) Plot of control and composite response using average material properties.

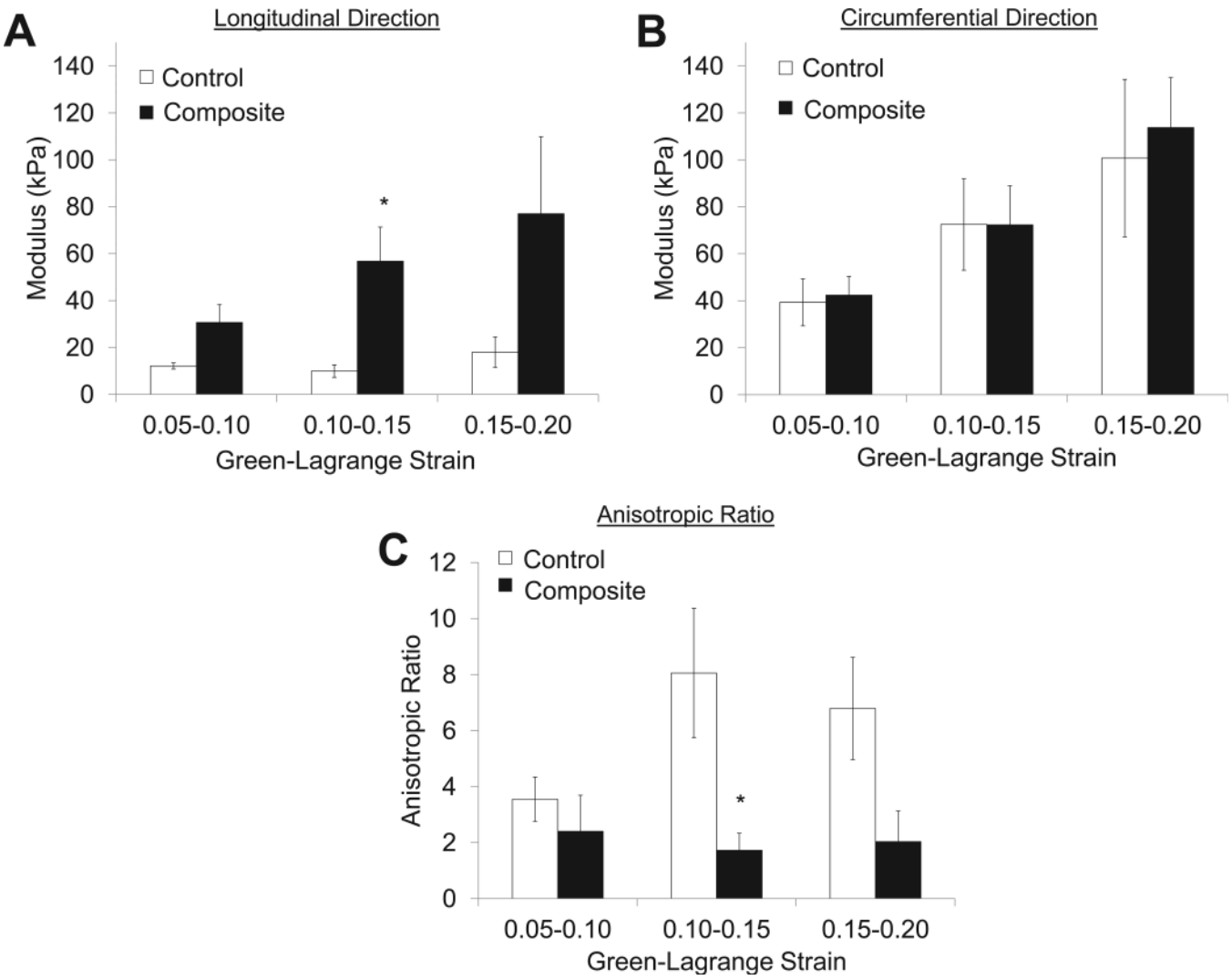

Figure 6.

Calculated moduli from tissue strains for control and composite samples in the (A) longitudinal and (B) circumferential directions, and (C) calculated anisotropic ratio. Data presented as mean ± SEM. *p<0.05 vs. control myocardium.

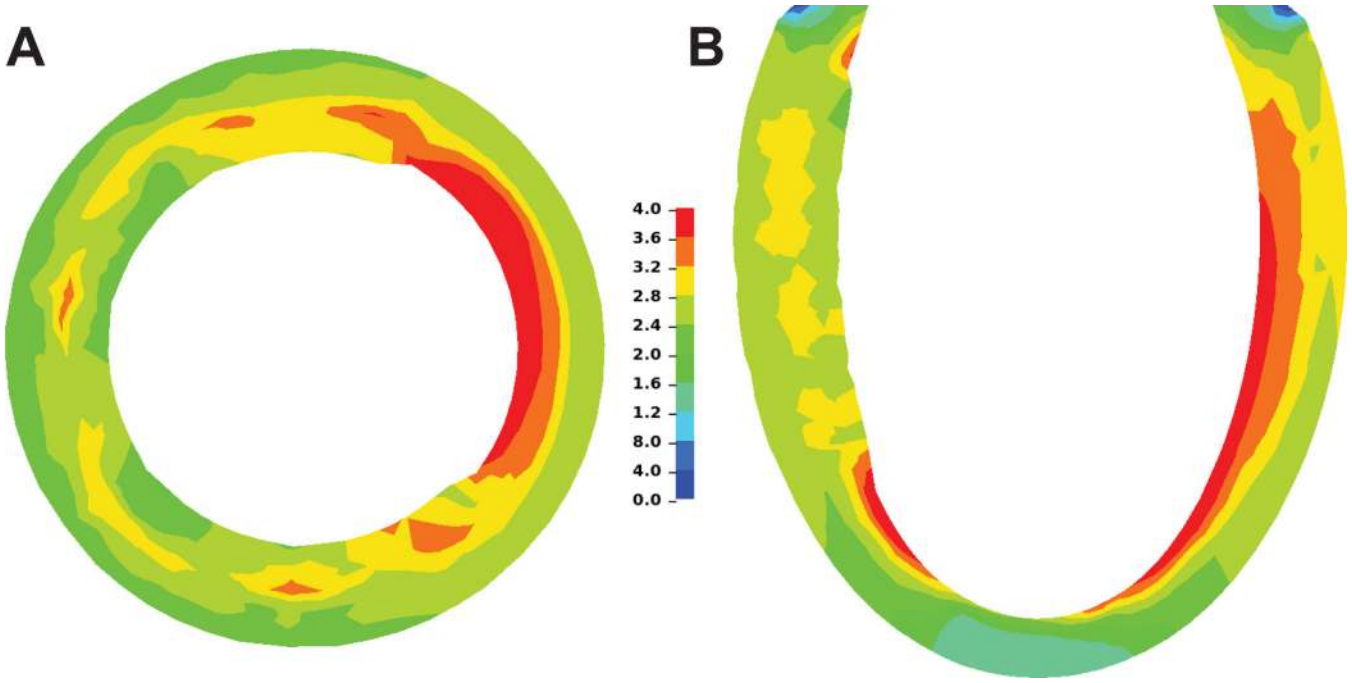

Figure 7.
Myofiber stress (kPa) distribution after hydrogel injection for the (A) short axis cross-section view located at mid-ventricle and (B) long axis cross-section view.

Table 1

Curve fitting results of biaxial testing data from (A) control, (B) composite, and (C) average of each case.

(A)					
Sample #	**C (kPa)**	**b_f**	**b_t**	**R^2 (circ)**	**R^2 (long)**
1	0.656	25.44	4.604	0.995	0.995
2	0.817	14.85	1.876	0.988	0.951
3	0.859	28.73	3.217	0.994	0.989
4	0.597	20.20	3.018	0.995	0.965
5	0.470	15.63	4.017	0.988	0.966

(B)					
Sample #	**C (kPa)**	**b_f**	**b_t**	**R^2 (circ)**	**R^2 (long)**
1	1.179	17.28	9.154	0.996	0.996
2	0.907	8.862	7.731	0.993	0.991
3	0.859	17.87	6.533	0.987	0.970
4	0.484	28.46	4.831	0.981	0.906
5	0.667	15.52	7.527	0.997	0.995

(C)			
Case	**C (kPa)**	**b_f**	**b_t**
Control	0.679±0.160	20.97±6.05	3.346±1.04
Composite	0.819±0.262	17.60±7.05	7.155±1.60

Table 2

End-diastolic myofiber stress averaged over different regions.

Case	Global kPa (% diff)	Circumferential kPa (% diff)	Longitudinal kPa (% diff)	Transmural kPa (% diff)
Control	2.89	3.35	3.04	3.37
Composite	2.49 (−13.9%)	2.75 (−18.1%)	2.38 (−21.9%)	2.49 (−26.0%)
Composite w/ control props	2.59 (−10.4%)	2.85 (−14.9%)	2.48 (−18.4%)	2.70 (−19.9%)